JOURNAL OF AIRCRAFT
Vol. 45, No. 4, July–August 2008

Effects of Wake Rollup on Formation-Flight Aerodynamics

Götz Bramesfeld* and Mark D. Maughmer†
Pennsylvania State University, University Park, Pennsylvania 16802

DOI: 10.2514/1.33821

The aerodynamic performance of two high aspect-ratio wings flying in formation is investigated with particular interest in the importance of considering wake rollup in making aerodynamic predictions. For this purpose, formations of various separations were investigated using a drag-free, fixed-wake model as well as a force-free, relaxed one. In all cases the aircraft were trimmed for roll and the follower aircraft pitch attitude was adjusted to match the lift coefficient of the lead aircraft. Both wake representations result in similar induced-drag minima for the follower aircraft which result when the lateral overlaps of the two aircraft are around 10% of a wingspan. Computations with the fixed-wake model, however, predict a wider region of lateral separations having the lowest induced drag than do the simulations with wake rollup. A small performance difference due to the wake model also exists when one aircraft follows directly behind the other. Independent of the wake model used, trimming the aircraft in roll and pitch can have a significant influence on their performance, although the required control-input solutions for trim are essentially not affected by the choice of wake representation.

Nomenclature

A, B, C	=	circulation coefficients
AR	=	aspect ratio
b	=	wingspan
C_{Di}	=	induced-drag coefficient
C_L	=	lift coefficient
D_i	=	induced drag
$D_{i\,\text{elliptical}}$	=	induced drag of elliptical load distribution
K	=	induced-drag factor: $D_i/D_{i\,\text{elliptical}}$
n	=	number of spanwise elements
Γ	=	circulation
γ	=	vorticity, $\mathrm{d}\Gamma/\mathrm{d}\eta$
Δi_{tip}	=	differential incidence angles of wing tips
Δx	=	streamwise separation
Δy	=	spanwise separation of aircraft centerlines
Δz	=	vertical separation
$\Delta\theta$	=	pitch adjustment
ξ, η, ζ	=	local reference frame

Introduction

FORMATION flight can increase the performance of a system of flight vehicles considerably as demonstrated by migrating birds [1–3]. A significant amount of effort can be saved by flying in the upwash field that exists outboard of the rolled-up tip vortices of a leading aircraft. The local upwash tilts the lift vector of the follower aircraft forward, thereby reducing its induced drag. A 10% power reduction has been reported for a Do-28 following a Do-228 [4], and up to 25% less drag than that of an isolated wing was measured in wind-tunnel tests for the follower of a two delta-wing formation [5]. The induced-drag reduction, however, is not limited to the follower aircraft alone. The lead aircraft is also subjected to the flowfield that the follower aircraft induces upstream with its bound and trailing-vortex system, although this influence decreases rapidly with increasing separation of the aircraft in the formation.

The gain in performance from formation flight comes without the structural and aeroelastic issues that often accompany similar gains achieved using high aspect-ratio wings. In addition, with modern flight-control systems, a close enough but safe spacing is now feasible such that the performance benefits of formation flight can be realized. An example of such a control system was demonstrated in flight tests with two F/A-18 research aircraft that flew in a close formation autonomously [6]. Under steady and level flight conditions, the formation-control system displayed lateral and vertical tracking performances that were within a few feet of the desired positions. The measured performance gain was a drag reduction for the follower aircraft of about 15%.

Most analytical investigations of formation flight rely on potential flow models, primarily because of the computational speed of these methods. They can be as simplistic as modeling each aircraft using a single horseshoe vortex [7] or as sophisticated as vortex-lattice methods [8,9] or full-panel codes. Lissaman [10] and King and Gopalarathnam [11] use exact solutions to determine the drag of formations in the Trefftz plane using complex-variable descriptions. All of these approaches use a fixed-wake model with prescribed shapes, although some work has been done with relaxed-wake schemes [12,13]. A relaxed-wake model can capture the secondary effects caused by the wake rollup, which can be significant when there is strong interaction between the lifting surfaces and their wakes, as is usually true for aircraft in formation flight. In that case, the wake of the lead aircraft may pass in close proximity of the wing of the trailing aircraft and can induce significant velocities there. Subsequently, the loads of the second aircraft to some extent depend on the amount of rollup that the lead-aircraft wake has experienced up to that point. A relaxed-wake model that models the rollup process is necessary to capture such secondary wake effects and accurately predict the induced loads.

The modeling of formation flight using a relaxed-wake model based on discrete vortex filaments can be numerically challenging due to the induced velocity being singular at the center of a filament. This can be a problem when the relaxation causes a trailing filament of the lead-aircraft wake to come into close proximity to a numerical control point of the follower aircraft. The resulting infinite or large velocities induced by the filament at that point can alter the flow situation considerably and, thus, have a disproportionate and unrealistic influence on the local circulation. A similar problem can arise when two or more wake filaments come into close proximity during the relaxation process. Because of the large velocities that they induce on each other, the filaments can experience relatively

Received 1 August 2007; revision received 7 November 2007; accepted for publication 9 November 2007.

*Visiting Assistant Professor, Department of Aerospace Engineering; currently Assistant Professor, Department of Aerospace and Mechanical Engineering, Saint Louis University, St. Louis, MO. Member AIAA.

†Professor, Department of Aerospace Engineering. Associate Fellow AIAA.

large displacements during a single time step and, as a result, the relaxation process can become numerically erratic. This erratic wake behavior is accentuated with an increased numbers of filaments along the span.

Although a viscous-core model eliminates any numerical issues related to the velocity singularity that occurs at the center of a filament, the arbitrary chosen core size becomes a driving factor of the solution. Although the core size has only limited impact on the induced drag of a single wing, it can have a strong influence where wakes interact closely with lifting surfaces, as is the case in formation flight. Obviously, the diameter of the solid core is what defines "close."

The research presented herein investigates the aerodynamic effects on formation flight that are due to wake rollup. For this purpose, a free-wake method is used to account for the bound circulation and the vorticity in the wake. Instead of using discrete filaments to model the wake, the method employed does so with elements composed of continuous vorticity distributions. By modeling the lifting surfaces and wakes with such elements, most of the singularity issues that are typical of discrete filament models are avoided. This approach is numerically well behaved and accurately predicts the aerodynamic loads despite strong interactions between wing and wake. Thus, the method supports the study of the influence of free- versus relaxed-wake models on the predicted loads and control requirements for a particular trimmed formation.

Theoretical Model

The flowfields of the cases presented herein were modeled using a potential flow method that relies on distributed vorticity elements. Although a more comprehensive discussion of this method can be found in [14,15], a brief description will be presented here. The key component of the method, the distributed vorticity element as depicted in Fig. 1, consists of vortex filaments along its leading and trailing edges. These filaments have spanwise circulation distributions that are parabolic and of opposite orientations. A vortex sheet having a linear spanwise vorticity distribution satisfies the Helmholtz-vortex theorems between these filaments. The vorticity of the sheet is aligned with the local ξ axes, which is oriented along the local flow direction. The sheet lies in the ξ–η plane, and the ζ axis is normal to the plane of the sheet.

Numerically, the velocity that such a distributed vorticity element induces at a given point is composed of the influences of two vortex filaments and two semi-infinite vortex sheets. As shown in Fig. 1, one vortex filament and one semi-infinite vortex sheet begin at the leading edge of the distributed vorticity element. The second set that has the opposite circulation and vorticity distribution begins at the trailing edge of the element. Consequently, the two vortex sheets cancel each other downstream of the trailing edge. The induced velocities of interest are computed using analytical solutions [14,16].

The advantage of using distributed vorticity elements to model a flowfield is that the two velocity components induced by a continuous vortex sheet are finite. One of the components is tangential to the plane of the sheet in the spanwise η direction, while the other one is normal to the plane of the sheet in the ζ direction. Although the spanwise velocity is singular in the plane of the vortex sheet, it remains finite up to it. Just on either side of the vortex sheet, the tangentially induced velocities are of equal magnitudes but in opposite directions. Thus for numerical purposes, the tangential velocity component that is induced in the plane of the sheet can be set to zero, which is the average of the values just above and below the plane of the sheet. The velocities that the vortex sheet induces normal to its plane are finite except along the edges of the sheet. For example, the normal velocity induced along the leading edge of the semi-infinite vortex sheet becomes singular if the leading edge is swept. Without sweep, however, the self-induced velocity along the leading edge is half the value that a doubly infinite vortex sheet would induce. Further singularities are present along the side edges of the sheet where the magnitude of the normal velocity component becomes infinite if the vorticity is nonzero.

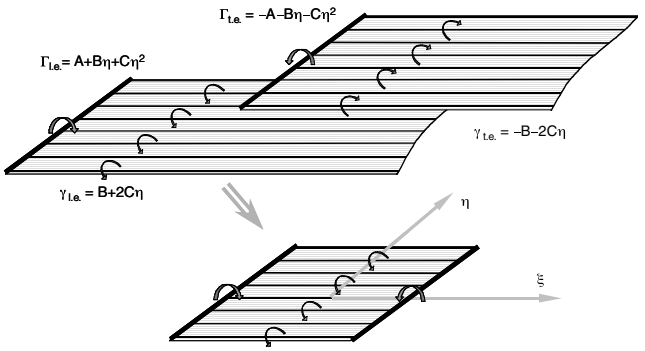

Fig. 1 A distributed vorticity element is composed of vortex filaments along its leading and trailing edges, as well as of two semi-infinite vortex sheets.

These singularities make the numerical implementation of a discretized model difficult. As the real flow is continuous and free of singularities, the summation of the discretized elements should yield the same. Thus, to handle the problem of the singularities numerically, they can be canceled mathematically by adding additional singularities along the edges of the element. When modeling a larger, continuous vortex sheet using distributed vorticity elements, the newly introduced singularities of two neighboring elements cancel each other as well. Consequently, the induced velocities of the entire flowfield remain unaltered by the discretized model with the exception of along the wing tip and at the outermost edges of the vortex sheet in the wake. If the vorticity is nonzero there, the newly introduced singularity will remain unbalanced. In that case, a forced limitation is imposed.

In the wake, the vortex filaments at the leading and trailing edges of a distributed vorticity element are omitted, because the streamwise vorticity in the wake remains constant with steady conditions at the lifting surface. Although this eliminates major line singularities in the wake, further singularities occur along a swept leading or trailing edge of the vortex sheet of a distributed vorticity element. These singularities are also handled by introducing additional ones in much the same way as those along the side edges of the element. Likewise, the overall sum of the added singularities does not alter the overall flowfield.

For the method employed, lifting surfaces are modeled using distributed vorticity elements in a manner similar to that used in the multiple lifting-line method of Horstmann [16]. In the spanwise direction, the parabolic circulation distributions of the vortex filaments form a second-order spline. The subsequent vortex sheets between the leading- and trailing-edge filaments form a continuous vortex sheet. Several such systems of vorticity filaments and vortex sheets can be arranged along the chord of the wing. Along the wing trailing edge, the parabolic vortex filament is omitted in order to satisfy the Kutta condition.

The normal force of a lifting surface is the sum of all the forces that arise from the Kutta–Joukowsky law being applied at the vortex filaments of each surface element. The force is composed of a part due to the freestream flow and one due to the induced velocities. The induced drag is computed along the trailing edge of each lifting surface. For this purpose, the Kutta–Joukowsky theorem is applied there using the spanwise circulation distribution and the velocity that the wake induces at the trailing edge of the lifting surfaces [17–19]. The wake shape is developed using a time-stepping method. As discussed in [14], the fixed-wake results obtained with this method agree well with those obtained using an analytical Trefftz-plane approach. This method of computing the drag is less sensitive to panel-density variations than are surface-pressure integration methods, or to the choice of the location of a "numerical Trefftz plane" for a drag integration in the far field. Furthermore, the approach used does not require a precisely described far-field wake shape to accurately determine the induced drag, as is the case for using a free-wake Trefftz-plane analysis.

Formation Flight

The free-wake, potential flow method described above is well suited for the investigation of the importance of free-wake effects on formation-flight aerodynamics. Of specific interest in this study is how the wake model used influences the aerodynamic loads on the aircraft, as well as how it affects the equilibrium or trim condition. The two models that are compared are a force-free wake that is relaxed and aligned with the local streamlines and a drag-free wake that is fixed and aligned with the freestream. The main interest is the effect of the wake model used on the induced-drag factor of each aircraft in the formation and on the longitudinal and lateral control solutions that are needed to maintain the formation. The induced-drag factor is the ratio of the induced drag of a wing to the equivalent elliptical circulation distribution. Thus, it is the reciprocal of the span-efficiency factor:

$$K = \frac{D_i}{D_{i\,\text{elliptical}}} = \frac{\pi\, AR\, C_{Di}}{C_L^2}$$

with AR being the aspect ratio of the wing. For a planar wing planform with a fixed wake, the theoretical limit of the induced-drag factor is unity.

In this study, a formation of two aircraft is investigated using fixed- and relaxed-wake models. Three iteration loops were required to obtain a converged wake shape, zero rolling moment, and equal lift coefficients for the two aircraft (thus assuming identical aircraft configurations). The wake was developed until the change in the induced-drag factor of the entire formation between two time steps was less than $\Delta K_{\text{formation}} = 0.0005$. In the case of a lateral offset in the formation, both aircraft must be trimmed in roll. In particular, the trailing aircraft can experience a significant rolling moment due to the asymmetrical velocity field induced by the wake of the lead aircraft. A similar, but smaller, rolling moment is induced on the lead aircraft by the trailing aircraft, although this interaction diminishes rapidly with increasing distance between the two aircraft. The rolling moments are zeroed by changing the incidence angle of the outer wing panels. As with an aileron deflection, the incidence angles are adjusted in opposite directions on the left and right outer panels. In addition to roll, the pitch attitude of the follower aircraft is adjusted to match the lift coefficients and, hence, speeds of the two aircraft.

Comparison with Experimental Results

A comparison between experimental and computational results is shown in Fig. 2. The experimental results were obtained from wind-tunnel tests using a formation of two wings with aspect ratios of 6.7 [20]. While a half-span model of the lead wing was mounted to the wind-tunnel wall and set to a fixed angle of attack, that of the full-span follower-model wing was varied and the resulting lift and drag forces measured. Although the formation configuration was designated as an echelon in [20], the test was effectively that of a symmetric three-aircraft formation with one lead aircraft that is followed by the full-span model and its mirror image. The three-wing configuration was considered in the computational simulations. Despite the rolling moment of the follower aircraft being recorded in the experiment, the formation was not trimmed in roll. For comparison with the computational results, experimental data with equal lift coefficients for the lead and follower aircraft were used. The measured drags were adjusted with the drag at zero lift of the base wing to account for viscous effects.

The performance results of the follower aircraft calculated with a relaxed, force-free wake agree well with the experimental results. Both methods predict similar minimum induced-drag factors of approximately $K = 0.25$ when the lateral separation of the fuselage centerlines is about 93% wingspans. This represents a significant performance increase over the baseline wing and its induced-drag factor of roughly 1.05. The computational results obtained with a fixed, drag-free wake indicate a higher minimum drag value, although low values extend over a wider range of lateral separations of the formation. The significant drag advantage predicted by the experiment for the formation with a lateral separation of 0.93 wingspans is, however, notably less for the computational results when the aircraft of the formation are trimmed in roll. In general, the drag variations due to roll trim are similar in magnitude to those due to the different wake representations. In any case, the relaxed-wake computational results agree well with those of the experiment when the conditions are the same.

Aircraft Formation

The aircraft used in this study are representative of high-aspect ratio, long-endurance aircraft. They are based on a modern high-performance sailplane that has a 15-m span. Its high aerodynamic efficiency makes it well suited for the investigation of relatively small aerodynamic effects. Various separations of a two-aircraft formation are investigated.

The aircraft wings have an aspect ratio of 22 and a dihedral of 3 deg. The wing planform consists of two trapezoids for each half-span with a taper break at about 60% of the half-span. The outer wing panel has 1.5 deg washout and serves as the "aileron" for roll trim. Each aircraft wing was modeled with 20 spanwise and one chordwise distributed vorticity elements. As shown in Fig. 3, fewer spanwise elements cause only small differences in the computed results for the induced-drag factors of the formation with varying lateral separations. In the wake, the streamwise length of the distributed vorticity elements is 2.7% of the span. Several streamwise, lateral, and vertical separations of the formation are assessed at lift coefficients of approximately 0.58 and 1.1, of which the smaller value is slightly less than the lift coefficient corresponding to the best lift-to-drag ratio of the aircraft.

Induced-Drag Results

The induced-drag factors of the two aircraft as they depend on the lateral spacing of the formation, calculated using the relaxed-wake model, are shown in Fig. 4. The results of three streamwise separations are shown in this figure. As expected, the formations have the poorest performances when the following aircraft is entirely

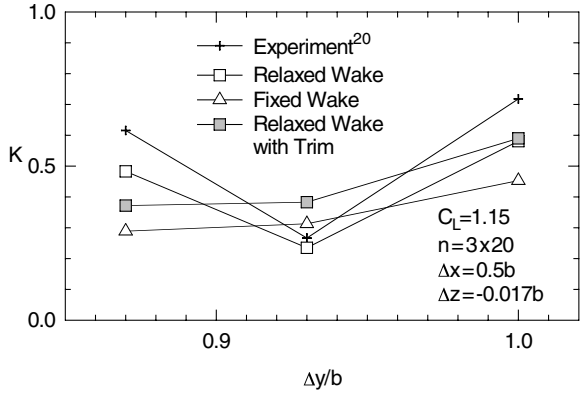

Fig. 2 Comparison of experimental and computational results of the performance of a follower wing in a three-wing formation.

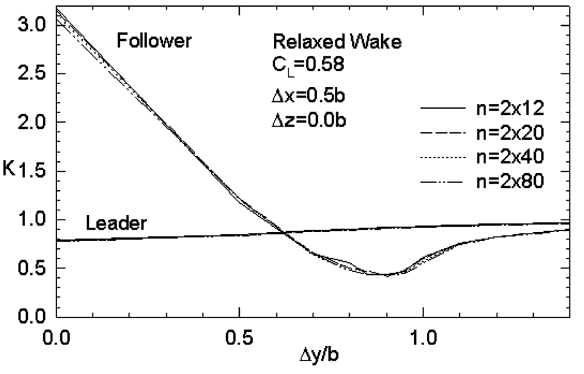

Fig. 3 Influence of varying spanwise panel density on the performances of two aircraft flying in formation.

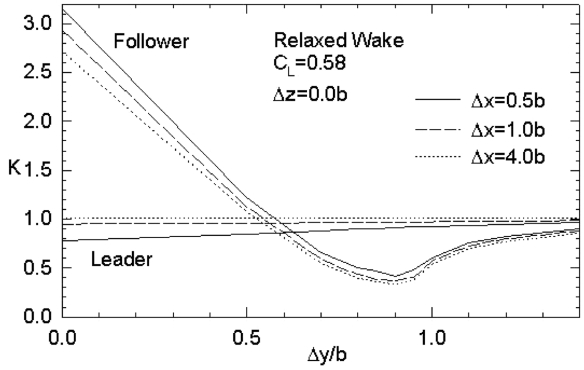

Fig. 4 The induced-drag factor variation due to changing lateral spacings of two aircraft flying in formations with three different separations in the streamwise direction: relaxed, force-free wake model.

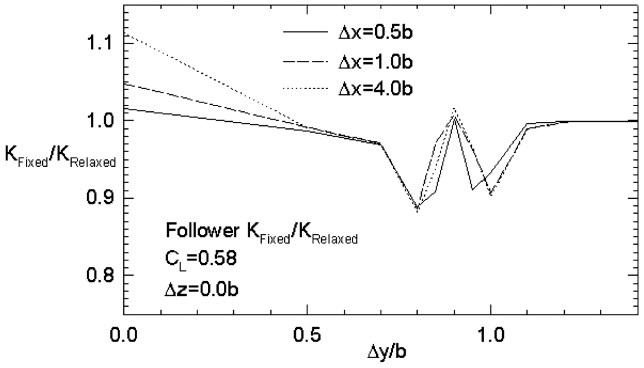

Fig. 6 The ratio of the fixed- to relaxed-wake induced-drag factors for the follower aircraft as it depends on lateral and streamwise spacing.

in the wake of the leader. In this particular case, the lead aircraft, which has an induced-drag factor of slightly less than 1, has slightly less induced drag than the baseline wing. This result is due to the induced upwash of the bound circulation of the follower aircraft, which diminishes with increasing streamwise separation in the formation. The follower-aircraft induced-drag factor is slightly above 3.0 when it is directly behind the leader, with variations due to streamwise separation. This value improves considerably as the aircraft move apart in the spanwise direction. The induced-drag factor of the trailing aircraft reaches its lowest values at a lateral spacing of the fuselages of about 90% wingspans, corresponding to a 10% span overlap of the wings. The minimum depends on the streamwise separation, with the lowest value occurring at a streamwise separation of four spans. Here, the downwash due to the bound circulation of the lead aircraft has the least effect on the trailing aircraft. The differences due to the streamwise separation diminish as the spanwise spacing is increased further and the induced-drag factor of the follower aircraft increases, approaching the value of the wing-alone case. Although the lead-aircraft performance improves slightly at certain separations, the follower aircraft is the primary beneficiary of the formation-performance gains.

The results of using a fixed-wake model on the same formation separations of the previous figure are shown in Fig. 5. Although the lead-aircraft performance is affected by the streamwise separation, it is not affected by the choice of wake model. For the trailing aircraft, the major difference for the fixed-wake calculation is that the lowest induced-drag factors stretch over a wider range of lateral spacings than they do in the relaxed-wake case. Further differences due to the wake model are apparent for the formation without lateral separation, where the fixed-wake model predicts slightly higher drag values.

Independent of the wake model, the effect due to the streamwise separations is primarily due to the influence of the bound circulations. For example, as the formation moves apart in the streamwise and spanwise directions, the influence of trailing-wing upwash on the lead aircraft diminishes. Similarly, the decreasing influence of the downwash induced by the bound circulation of the lead wing on the performance of the trailing wing is reduced as the formation moves apart and the differences between the streamwise separations diminish as wake effects become predominant. The wake effects are essentially identical for the chosen streamwise separations, which is in line with the findings of [21], in which the majority of the shed vorticity becomes concentrated in the tip vortices within one or two chord lengths aft of the trailing edge of a wing. Thus, half a span aft of the lead-aircraft trailing edge, the majority of the shed vorticity is already accumulated in the tip vortex. To a limited extent, Munk's stagger theorem [22], which states that the overall induced drags of the fixed-wake results are independent of the streamwise separation and depend solely on the spanwise circulation distributions, also holds true for the relaxed-wake results once the majority of the vorticity is rolled up in the tip vortex. Although not captured by potential flow models, viscous effects, although relatively small, are of increasing importance with distance from the trailing edge in that they cause dissipation in the wake.

To illustrate the differences in induced-drag prediction for the two wake models, the ratios of the follower-aircraft induced-drag factors for the fixed- and relaxed-wake models are plotted in Fig. 6. The differences in the predictions based on the two wake models only vary slightly with streamwise spacing except when the follower aircraft is directly behind the lead aircraft. In this case, as the streamwise separation increases, the influence of the wake shed from the lead aircraft becomes increasingly greater than that of its bound circulation and, thus, differences between the fixed- and relaxed-wake results increase. Other significant differences due to the wake model exist near the performance peak at lateral spacings around 90% wingspans. These differences reflect the somewhat wider low-drag range predicted using the fixed-wake model than found using the relaxed-wake model.

The largest performance differences due to the wake model exist when the tip regions of the wakes interact, for example, as shown in Fig. 7. This figure shows the shapes of the computed, free-wake

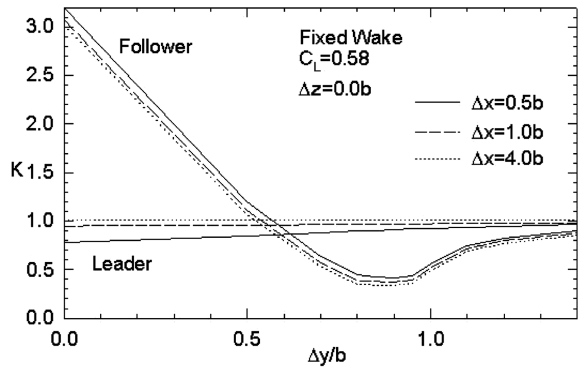

Fig. 5 The induced-drag factor variation due to changing lateral spacings of two aircraft flying in formations with three different separations in the streamwise direction: fixed, drag-free wake model.

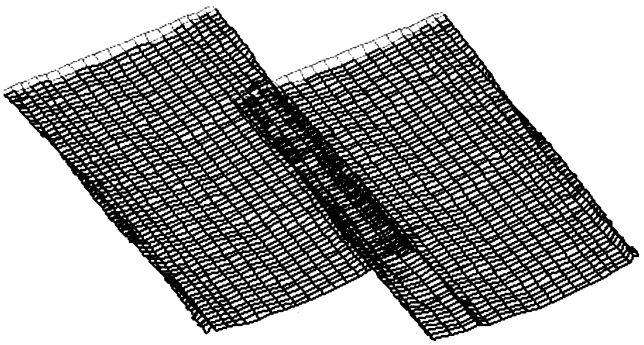

Fig. 7 The wake-vortex sheets that are shed by the wings of a formation with a streamwise separation of $\Delta x = 0.5b$ and lateral spacing of $\Delta y = 0.8b$.

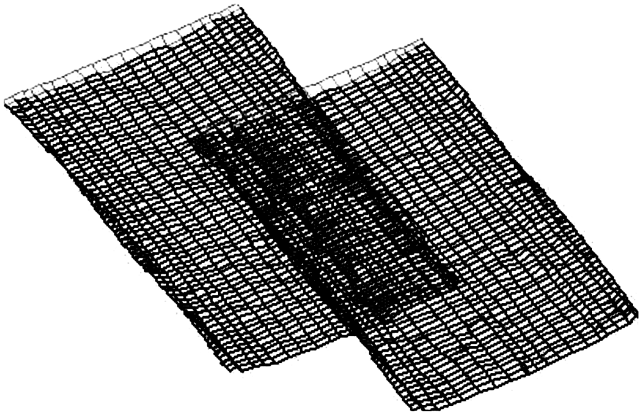

Fig. 8 The wake-vortex sheets that are shed by the wings of a formation with a streamwise separation of $\Delta x = 0.5b$ and lateral spacing of $\Delta y = 0.5b$.

sheets shed by the two-wing formation with a lateral spacing of $\Delta y = 0.8b$ and a streamwise separation of $\Delta x = 0.5b$. As can be observed in Figs. 4 and 5, a more extreme overlap of the two wingspans does not necessarily result in significant differences in predicted drag factors due to the wake model, even when a strong interaction exists between the vortex sheets. An example is a lateral spacing of $\Delta y = 0.5b$, whose computed free-vortex sheets are shown in Fig. 8. Despite the obvious strong interaction, the induced-drag factors calculated for both wake models are essentially equal.

The induced-drag factors for a formation whose aircraft operate at higher lift coefficients than in the previous case, $C_L = 1.1$, are shown in Figs. 9 and 10 for predictions obtained using relaxed- and fixed-

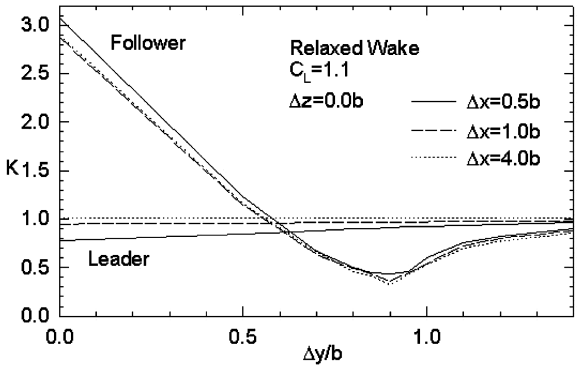

Fig. 9 The induced-drag factor variation due to changing lateral spacings of two aircraft flying in formations with three different separations in the streamwise direction: relaxed, force-free wake model.

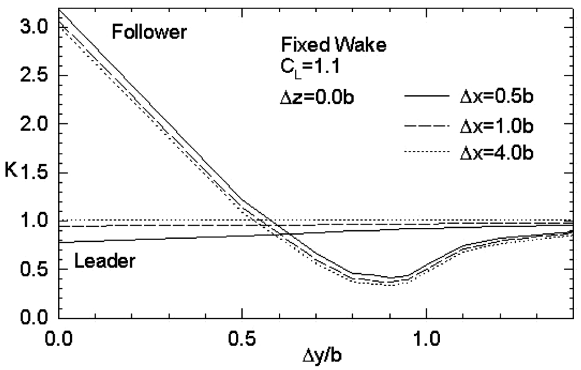

Fig. 10 The induced-drag factor variation due to changing lateral spacings of two aircraft flying in formations with three different separations in the streamwise direction: fixed, drag-free wake model.

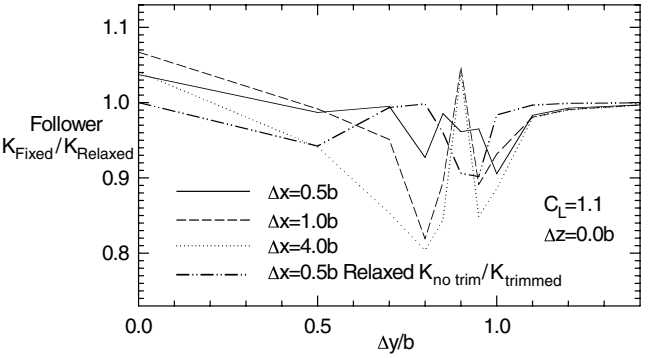

Fig. 11 The ratio of the fixed- to relaxed-wake induced-drag factors for the follower aircraft as it depends on lateral and streamwise spacing. Additionally shown is the ratio of the induced-drag factors of the formation with and without roll trim.

wake models, respectively. Although the fixed-wake predictions are nearly identical to those obtained at lower lift coefficients due to the linear nature of the theory, the relaxed-wake models differ slightly due to the different amounts of rollup of the lead-aircraft wake-vortex sheet at the two lift coefficients. Consequently, the induced-drag ratios of the two wake models presented in Fig. 11 deviate more from unity than those obtained at the lower lift coefficients. These differences are more pronounced with the larger streamwise separations, indicating the changing influence of the increased amount of wake rollup for a given streamwise separation relative to the amount of influence of the bound circulation of the lead aircraft. Despite the differences of the two wake models, both predict the lowest induced-drag factors at about 90% wingspans lateral spacings and agree within a few percent.

To assess the effect of the vertical separation of the formation on the performance of the follower aircraft, contours of its induced-drag factor are plotted in Fig. 12. Vertical separations of ±35% span and lateral separations of the fuselages of 50 to 120% span are surveyed for a formation with a one-span streamwise separation, each aircraft operating at $C_L = 1.1$. The results of $\Delta z/b = 0$ correspond to those plotted in Figs. 9 and 10 for the respective streamwise separations of the formation.

Very little difference exists between the contours of the two different wake models. The primary differences exist near and slightly inboard of the performance peak of zero vertical separation. In these regions, the fixed-wake model predicts more optimistic induced drags, as already reflected in the results presented in Fig. 11. Any increase in vertical separation essentially yields induced-drag values for the follower that are largely independent of the choice of wake model.

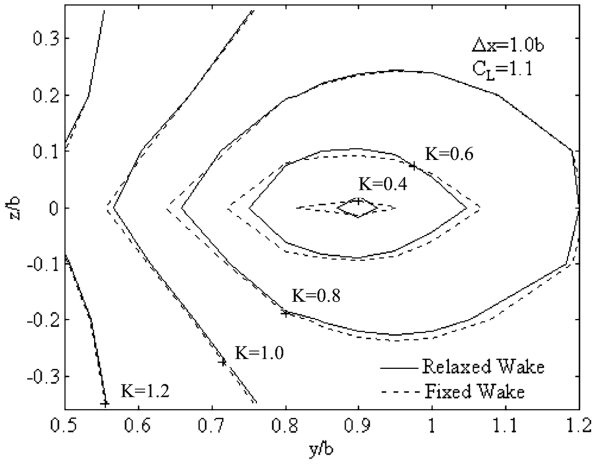

Fig. 12 Comparison of induced drag-factor contours of the follower aircraft of formation of a streamwise separation of one span using a fixed- and a relaxed-wake model.

Trim Results

As evident from the results presented in Fig. 2, the induced-drag factor of the follower aircraft in a formation can be noticeably influenced by the control inputs that are needed to compensate for the rolling moment resulting from the interaction with the lead-aircraft wake. A similar behavior is also observed for the higher aspect-ratio wings that were used in this study. In addition to the ratios of the induced-drag factors of fixed- and relaxed-wake models, the analogous ratios of the wings with and without trim in roll are shown in Fig. 11. A relaxed-wake representation was used in both cases. The ratios are nearly unity for most of the lateral-formation separations, in particular with zero lateral separation, which requires no roll correction. Significant differences, however, exist near the performance peak of the 90 to 95% span lateral separation.

With the exception of the no-trim results of Fig. 11, the drag results presented were computed with lead and follower aircraft trimmed in roll. Trim is achieved by changing the incidence angles of the outer 40% span of each wing panel in opposite directions, as would be the case with an aileron deflection. According to thin airfoil theory, a 1 deg change of differential incidence angle is approximately equivalent to a 1.8 deg deflection of a 20% chord. In addition to trim in roll, the follower-aircraft pitch attitude was adjusted so that it matched the lift coefficient of the lead aircraft.

The required control inputs for trimmed formations as they depend on the lateral separation of the two aircraft are plotted for streamwise separations of half a span in Fig. 13 and for four spans in Fig. 14. These results are for aircraft-lift coefficients of 0.58. The differential incidence angles and pitch adjustments for the follower aircraft are presented for predictions obtained using both fixed- and relaxed-wake models.

For the half-span streamwise separation, the predicted pitch-control inputs are essentially identical for the fixed and relaxed-wake models. The fixed-wake model predicts that a slightly larger pitch

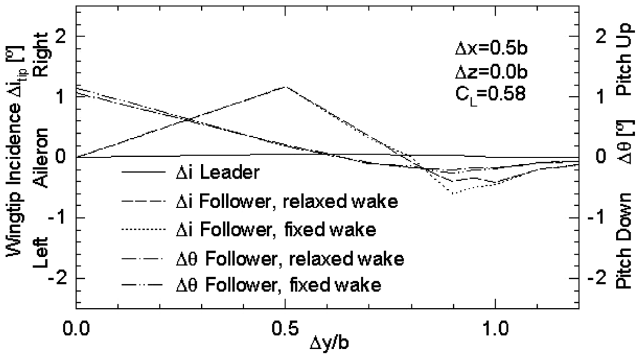

Fig. 13 The required control inputs for trimmed flight of the two-aircraft formation, half a span apart in the streamwise direction, with different spanwise staggers.

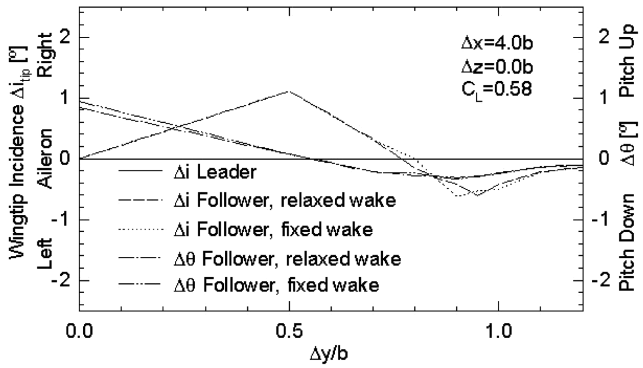

Fig. 14 The required control inputs for trimmed flight of the two-aircraft formation, four spans apart in the streamwise direction, with different spanwise staggers.

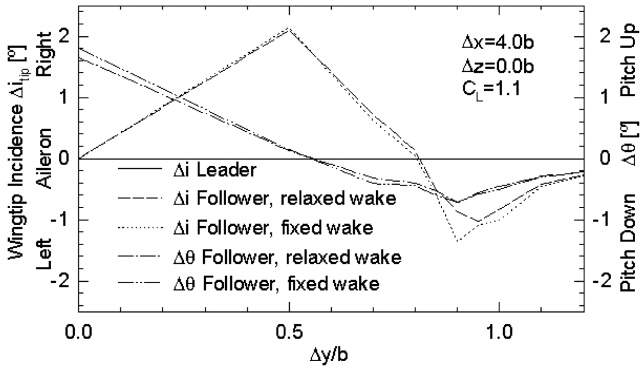

Fig. 15 The required control inputs for trimmed flight of the two-aircraft formation, four spans apart in the streamwise direction, with different spanwise staggers.

correction is needed to adjust for the downwash of the lead aircraft, an effect that is apparently reduced as the shed wake-vortex sheet rolls up. In roll, the control solutions of the two wake models are the same except in the region of the greatest performance benefit. There, the fixed-wake model predicts a larger corrective input for the follower aircraft than does the relaxed-wake model. As with the pitch correction, the rollup of the wake appears to reduce the impact of the lead-aircraft wake. For the four-span streamwise separation case, the control required to trim in roll is essentially unchanged from the half-span case. As expected, the roll corrections required by the lead aircraft are small and, essentially, independent of the wake model, yet depend on the streamwise separation. The small amount of "right aileron" that is required to compensate for the upwash field induced by the bound vorticity of the follower aircraft becomes essentially zero at larger streamwise separations.

Although aircraft of a formation operating at lift coefficients of 1.1 require larger trim adjustments, as shown in Fig. 15 for a formation with a four-span streamwise separation, the general behavior of these control inputs is very similar to those presented for the lower lift coefficients. For example, at a lateral spacing of half a span, the increase of differential incidence adjustment of nearly 2.2 deg is proportional to the increase in vorticity shed by the lead aircraft. Furthermore, the differences between the two wake models appear to be largely independent of the lift coefficient. Where differences exist, they appear to be due to the reduction of the effect that the rolled-up wake of the lead aircraft has on the wing of the follower aircraft.

Circulation Distribution

Independent of the wake model used, the detrimental effect of the relatively large roll correction by the follower aircraft in the $\Delta y = 0.5b$ formation is apparent in the spanwise circulation distributions that are plotted in Fig. 16. This figure shows the normalized spanwise

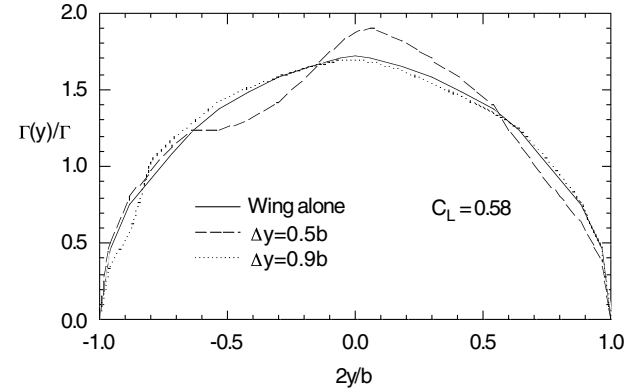

Fig. 16 The normalized, spanwise circulation distributions of the following aircraft of a two-aircraft configuration with varying lateral spacing and a half-span streamwise separation.

circulation distributions of the base wing alone, as well as those of the trailing aircraft in formations with lateral spacings of 0.5 and 0.9 span. The large changes in spanwise circulation distribution for the $\Delta y = 0.5b$ formation results in a relatively large induced-drag penalty. Additionally, the spanwise variation of the induced drag results in an adverse yawing moment. Although not considered in the results discussed here, the rudder input for compensating the adverse yaw would result in additional drag and compound the performance penalty of that particular formation.

In contrast to the previous case, the trailing aircraft of the formation with a lateral spacing of $\Delta y = 0.9b$ benefits from the upwash field of the lead-aircraft wake without the need of large aileron inputs. Likewise, its adverse yaw penalty is also much smaller, as demonstrated by the spanwise lift distribution in Fig. 16. The lift distribution is, in fact, relatively close to that of the base wing. In addition to the greater performance gain, the larger spacing of this formation ensures a safer operation than would the closer formation.

Conclusions

In considering the predicted results obtained using fixed- and relaxed-wake models, both yield similar values for the induced-drag factor of the follower aircraft in a two-aircraft formation. An exception is in the region of the lowest induced-drag factors, for which the fixed-wake model predicts a wider range of lateral-formation separations than does the relaxed-wake model. In the relaxed-wake case, the lowest drag values, for an overlap of approximately 10% of the aircraft spans, are restricted to a much narrower region of lateral-formation separations. Small differences also exist in the computed trim solutions that are required to keep the formation in level flight, particularly in the region of the greatest performance benefit. In general, however, the use of either wake model gives very similar performance and trim solutions. In fact, having the aircraft trimmed in roll or not appears to have an effect on the performance that is at least as significant as that of the choice of wake model. Nevertheless, if a high level of accuracy is required, especially in the region of the best performance benefit, it appears to be advisable to use the relaxed-wake model. The advantage of the fixed-wake model, however, is that it requires considerably less computational effort, which might be significant, for example, if the loads are needed as part of a broader simulation.

Acknowledgments

The thoughtful comments and insights provided by J. Douglas McLean of Boeing Commercial Airplane Group are gratefully acknowledged.

References

[1] Lissaman, P. B., and Shollenberger, C. A., "Formation Flight of Birds," *Science*, Vol. 168, May 1970, pp. 1003–1005. doi:10.1126/science.168.3934.1003

[2] Hummel, D., "Aerodynamic Aspects of Formation Flight in Birds," *Journal of Theoretical Biology*, Vol. 104, No. 3, Oct. 1983, pp. 321–347. doi:10.1016/0022-5193(83)90110-8

[3] Hainsworth, F. R., "Precision and Dynamics of Positioning by Canada Geese Flying in Formation," *Journal of Experimental Biology*, Vol. 128, March 1987, pp. 445–462.

[4] Beukenberg, M., and Hummel, D., "Aerodynamic Performance and Control of Airplanes in Formation Flight," ICAS Paper 90-5.9.3, 9–14 Sept. 1990.

[5] Blake, W. B., and Gingras, D. R., "Comparison of Predicted and Measured Formation Flight Interference Effects," *Journal of Aircraft*, Vol. 41, No. 2, March–April 2004, pp. 201–207.

[6] Hanson, C. E., Ryan, J., Allen, M. J., and Jacobson, S. R., "Flight Test Results for an Autonomous Formation Flight Control System," AIAA Paper 2002-3431, May 2002.

[7] Blake, W., and Multhopp, D., "Design, Performance and Modeling Considerations for Close Formation Flight," AIAA Paper 1998-4343, Aug. 1998.

[8] Iglesias, S., and Mason, W. H., "Optimum Spanloads in Formation Flight," AIAA Paper 2002-0258, Jan. 2002.

[9] Maskew, B., "Formation Flying Benefits Based on Vortex Lattice Calculations," NASA CR-151974, May 1977.

[10] Lissaman, P. B., "Simplified Analytical Methods for Formation Flight and Ground Effect," AIAA Paper 2005-851, Jan. 2005.

[11] King, R. M., and Gopalarathnam, A., "Ideal Aerodynamics of Ground Effect and Formation Flight," *Journal of Aircraft*, Vol. 42, No. 5, Sept.–Oct. 2005, pp. 1188–1199.

[12] Wang, Z., and Mook, D., "Numerical Aerodynamic Analysis of Formation Flight," AIAA Paper 2003-610, Jan. 2003.

[13] Han, C., and Mason, W. H., "Inviscid Wing-Tip Vortex Behavior Behind Wings in Close Formation Flight," *Journal of Aircraft*, Vol. 42, No. 3, May–June 2005, pp. 787–788.

[14] Bramesfeld, G., "A Higher Order Vortex-Lattice Method with a Force-Free Wake," Ph.D. Dissertation, Pennsylvania State University, University Park, PA, Aug. 2006.

[15] Bramesfeld, G., and Maughmer, M. D., "A Relaxed Wake Vortex-Lattice Method Using Distributed Vorticity Elements," *Journal of Aircraft*, Vol. 45, No. 2, March–April 2008, pp. 560–568. doi:10.2514/1.31665

[16] Horstmann, K. H., "Ein Mehrfach-Traglinienverfahren und seine Verwendung für Entwurf und Nachrechnung nichtplanarer Flügelanordnungen," Ph.D. Dissertation, DVFLR, Institut für Entwurfsaerodynamik, Braunschweig, Germany, DFVLR-FB 87-51, Dec. 1987.

[17] Eppler, R., "Die Enwicklung der Tragflügeltheorie," *Z. Flugwissenschaft*, Vol. 11, 30. Ludwig-Prandtl-Gedächtnisvorlesung, Stuttgart, Germany, April 1987, pp. 133–144.

[18] Mortara, K. W., and Maughmer, M. D., "A Method for the Prediction of Induced Drag for Planar and Non-Planar Wings," AIAA Paper 93-3420-CP, Aug. 1993.

[19] Eppler, R., and Schmidt-Göller, S., "A Method to Calculate the Influence of Vortex Roll-Up on the Induced Drag of Wings," *Finite Approximations in Fluid Mechanics II*, Notes on Numerical Fluid Mechanics, DFG Priority Research Programme Results 1986–1988, Vol. 25, Vieweg Sohn, Braunschweig/Wiesbaden, Germany, 1989, pp. 93–107.

[20] Bangash, Z. A., Sanchez, R. P., and Ahmed, A., "Aerodynamics of Formation Flight," *Journal of Aircraft*, Vol. 43, No. 4, July–Aug. 2006, pp. 907–912.

[21] McCormick, B. W., Tangler, J. L., and Sherrieb, H. E., "Structure of Trailing Vortices," *Journal of Aircraft*, Vol. 5, No. 3, May–June 1968, pp. 260–267.

[22] Munk, M. M., "Minimum Induced Drag of Aerofoils," NACA, TR 121, 1921.